Punching Shear Behavior of FRP RC Flat Slabs Part 1: Experimental Study

Abdel Wahab El-Ghandour[1], Kypros Pilakoutas[2] and Peter Waldron[3]

Abstract: This paper presents the results of a two-phase experimental program investigating the punching shear behavior of FRP RC flat slabs with and without CFRP shear reinforcement. In the first phase, problems of bond slip and crack localization were identified. Decreasing the flexural bar spacing in the second phase successfully eliminated those problems and resulted in punching shear failure of the slabs. However, CFRP shear reinforcement was found to be inefficient in enhancing significantly the slab capacity due to its brittleness. A model, which accurately predicts the punching shear capacity of FRP RC slabs without shear reinforcement, is proposed and verified. For slabs with FRP shear reinforcement, it is proposed that the concrete shear resistance is reduced, but a strain limit of 0.0045 is recommended as maximum strain for the reinforcement. Comparisons of the slab capacities with ACI 318-95, ACI 440-98 and BS 8110 punching shear code equations, modified to incorporate FRP reinforcement, show either overestimated or conservative results.

Keywords: Punching shear; Flat slabs, FRP reinforcement; GFRP, CFRP, Shear reinforcement; Design equations

[1] Researcher, The University of Sheffield (Currently Lecturer, Ain Shams University, Egypt)
[2] Reader, The University of Sheffield, Department of Civil and Structural Engineering
[3] Professor, Pro-vice Chancellor, The University of Sheffield, Department of Civil and Structural Engineering, Centre for Cement and Concrete, Mappin Street, Sheffield, S1 3JD, UK

INTRODUCTION

In many parts of the world, corrosion of steel reinforcement in concrete structures is a major durability problem, leading to structural degradation and consequent costly repairs and loss of use. In the past decade, the use of advanced composites, normally called fiber reinforced polymers (FRP), as reinforcement for concrete structures has emerged as one of the most promising new technologies in construction to overcome the problem of corrosion.

Some of the most important elements that suffer from corrosion in concrete structures are slabs, as they represent the largest portion of any structure exposed to the environment. Furthermore, using FRP reinforcement, instead of steel, may result in a reduction in the concrete cover, which, in the case of slabs, represents a very substantial portion of the cross-section. Nevertheless, before the introduction of FRP into the construction industry, research needs to be done for the development of an understanding of the behavior of FRP RC flexural elements, including flat slabs. In this respect, an extensive experimental and theoretical study was conducted at the Centre for Cement and Concrete of the University of Sheffield to investigate the punching shear behavior of FRP RC flat slabs [El-Ghandour (1999)]. This work was initiated during a Pan-European project called Eurocrete (which developed the Eurocrete bar) and continues under the EU TMR (Training and Mobility of Researchers) research network Confibrecrete. This paper presents the experimental phase of the study including the experimental work, key experimental results and the most important conclusions derived. Punching shear design guidelines for FRP RC flat slabs with and without FRP shear reinforcement are also presented.

EXPERIMENTAL PROGRAM

Testing arrangement and design of the slabs

In this study, the testing arrangement adopted is similar to that used in tests undertaken previously at Sheffield [Li (1997) and Pilakoutas et al (1999)], using an existing rig for loading flat slabs, as shown in figure 1. The slab is supported through a column stub on a beam reacting against two reaction ring frames. Equal point loads are applied downwards symmetrically at eight locations on a circle of diameter 1.7 meters. The loading arrangement roughly corresponds to the circle of contraflexure over a column in an equivalent 4 meter uniformly distributed continuous span, or a 6 meters prototype span. Eight hydraulic jacks of 100 kN capacity are used for this purpose. The eight jacks are connected to the same pump, so that each jack applies the same load to the specimen.

Due to the uncertainty of dealing with new materials, the flexural capacity of the slabs of the first phase was designed not to exceed 50 % of the rig strength. For the slabs of the second phase, the flexural and punching shear designs were carried out based on the experience gained from the first phase of testing. The ultimate design moment of the slabs, M_{design}, was determined according to the calculated least resistance plane of flexural failure as shown in figure 1, [El-Ghandour, Pilakoutas and Waldron (1997, 1998 and 1999b)]. The yield line theory was not used in the design due to the lack of potential ductility expected in the case of FRP reinforcement. All the checks for punching shear, as well as the design of shear reinforcement were made according to the BS 8110 (1985) code requirements, taking into consideration the modifications to incorporate

non-ferrous reinforcement proposed by the Institution of Structural Engineers in the UK (1999) and Clarke (1996) for the Eurocrete project [Sheard et al (1997)]. These modifications are discussed later.

Slab details

The slabs of the first phase were given codes SG1, SC1, SGS1 and SCS1, and of the second phase SG2, SG3, SC2 and SGS2. Roughly equal areas of reinforcement were used during each phase for Glass and Carbon FRP bars. The slab geometry and reinforcement is shown in figures 2 and 3. The slabs were reinforced with top flexural reinforcement mats of round and square Eurocrete bars. These bars have a rough surface, which results in 'good' bond characteristics [Achillides et al., (1997)], roughly equivalent to those of ribbed steel. Slabs coded SG and SC were reinforced in flexure with glass (E_{FRP} 45 GPa, f_{FRP} 800 MPa) and carbon (E_{FRP} 110 GPa, f_{FRP} 1400 MPa) FRP bars, respectively, but had no shear reinforcement. Slabs coded SGS and SCS were similarly reinforced in flexure, but had carbon FRP shear reinforcement. The average cube compressive strengths from control specimens cast along side each of the slabs are shown in table 1.

Shear reinforcement was provided by the "Shearband" system developed at Sheffield [Li and Pilakoutas, (1995)], but using CFRP strip instead of steel. The dimensions and shape of the "Shearband" are shown in figure 2. The distribution and positioning of the shear reinforcement above the top flexural bars of the SGS and SCS slabs is shown in figure 3.

Loading and Instrumentation

One load cycle was applied at around 150 kN load, before loading to failure. This loading regime enables the detection of any significant damage at the service load level. Extensive measurements were made of strains on key locations on the flexural and shear reinforcements. Linear voltage displacement (LVD) transducers were also used to measure the vertical and horizontal deflections as well as concrete strains.

EXPERIMENTAL RESULTS

Bond slip and crack localization in slabs SG1 to SCS1

The first four slabs with low reinforcement ratio failed in a pseudo-flexural mode due to bond slip of the flexural bars. For these slabs, it was observed that the main cracks developed directly above the longitudinal reinforcement as shown in figure 4, partly because that is where a plane of concrete weakness exists. These cracks were very wide due to the low modulus of elasticity of the FRP reinforcement, as well as, the large spacing between the flexural bars. These triggered concrete splitting at higher loads on the top of all slabs close to the column and lead to the bond slip failure. This leads to the conclusion that one of the main advantages of using FRP reinforcement in slabs, which is to reduce the concrete cover, can lead to splitting problems and requires attention during design.

Instrumental evidence of bond slip failure was obtained from measurements which show that the average strains on the top concrete surface at failure are much higher (by up to 10 times) than the

maximum strains in the flexural bars, shown in figure 5. Bond slip failure is also responsible for the low flexural reinforcement strains in figure 5 (8300, 5000, 5800 and 3800 microstrains for slabs SG1, SC1, SGS1 and SCS1, respectively), confirming that only relatively low stresses compared to the strengths of the GFRP and CFRP materials were developed in the flexural reinforcement at failure.

Considering the strains in the shear reinforcement, it was noted (El-Ghandour, 2000) that only relatively low strains of 2600 and 4000 microstrains, corresponding to stresses of 286 and 440 MPa for slabs SGS1 and SCS1, respectively, were developed at failure. Again, this is attributed to the bond slip failure of the slabs, which precipitated the pseudo-flexural failure and resulted in the shear reinforcement not being fully activated. It should be noted that due to its shape, the shear reinforcement did not contribute much in preventing bond slip. The horizontal parts of the 'Shearband' were too close to the flexural bars to stop the crack initiation and the vertical legs are 50 mm away and, hence, provide no vertical confinement to the bar or the splitting stresses.

Punching shear failure of slabs SG2 to SGS2

Slabs SG2 to SGS2 failed in punching shear as shown in figure 6. Although the main cracks in these slabs developed directly above the longitudinal reinforcement, as in the first four slabs, the smaller bar spacing resulted in a larger number of cracks with smaller widths, leading to a much better crack distribution. This eliminated the problems of crack localization and concrete splitting, hence, preventing bond slip. It should be mentioned that the better horizontal

confinement provided by the larger number of bars in slabs SG2 to SGS2 has also contributed to this result.

From figure 7, it can be noted again that, for all four slabs, only relatively low strains and hence stresses, were developed in the flexural reinforcement at punching shear failure compared to the strengths of both GFRP and CFRP materials, although bond slip was prevented. This is attributed to the low stiffness FRP reinforcement which results in punching shear failure partly due to the loss of aggregate interlock resistance caused by the high strains developed in the reinforcement at low load levels. However, the strains developed in the flexural bars at punching shear failure are far beyond the limit value of 0.0025 (yield strain for conventional steel), adopted implicitly by the strain approach used in modified code equations.

Considering the strains in the shear reinforcement for slab SGS2 shown in figure 7 a maximum strain of 5900 microstrains is noted in the CFRP shear reinforcement at failure, corresponding to a stress of 649 MPa. Computing the average strain in the shear reinforcement at failure, a value of 4057 microstrains (average of strains in the punching perimeter), corresponding to an average stress of 446 MPa, is obtained. Although bond slip of the flexural bars was successfully prevented, it is obvious that lower stresses were developed in the shear reinforcement of this slab at punching shear failure compared to the strength of the CFRP material. This can be attributed to possible slippage of the shear reinforcement at failure, which can be detected by noting the strain reduction at constant load shown in figure 7. However, it should be noted that the average strain level of 0.0041 in the shear reinforcement is still far beyond the 0.0025 value of the yield strain of steel. Furthermore, the shear reinforcement strains in slab SGS2 showed that, only one layer of

shear reinforcement was fully activated, which means that adopting a maximum spacing of 0.75d, as in BS 8110 (1985), is unconservative. A reduced maximum spacing of 0.5d is hence proposed [El-Ghandour, Pilakoutas and Waldron (1999a)], in line with the ACI 318 (1995).

Displacement and ultimate capacity of the tested slabs

Considering figures 8 and 9 showing the load versus deflection curves at position D850 (average displacement at a radius of 850 mm from the center), it is obvious that the post-cracking portions of the load-deflection curves of slabs SG2 to SGS2 show a bigger increase in the load up to failure when compared to slabs SG1 to SCS1. This can be attributed to the higher reinforcement ratio of the former slabs. However, it should be noted that such stiffness is still much lower than the one normally expected from conventionally RC slabs. Nevertheless, it is obvious that the post-cracking behavior of the slabs with CFRP flexural reinforcement, is better than that of the GFRP flexurally reinforced slabs, since carbon bars have a higher elastic modulus.

Figures 8 and 9 also show that the SG slabs demonstrate higher deflections at failure and, hence, higher deformability than SC slabs. This is due to the lower modulus of elasticity of glass, resulting in a reduced effective moment of inertia of the SG slabs. In addition, larger deformability is also demonstrated in slabs with shear reinforcement compared to slabs without shear reinforcement. In the slabs of the first phase, the slight increase in deformability is attributed to the partial anchorage provided by the shear reinforcement to the flexural bars, which causes bond slip failure to occur at higher loads and deflections. However, in slab SGS2, the more significant increase in deformability could be attributed to the fact that, unlike in slabs SG2

and SG3 without shear reinforcement, a more flexible punching shear mechanism took place, due to the mobilization of its shear reinforcement before punching shear failure. This justifies the lower deformability of slab SG2 with higher concrete grade when compared to slab SGS2, although equal capacities are achieved. Finally, it should be noted that the slabs of the second phase demonstrate lower deformability when compared to the corresponding slabs of the first phase, as shown in figures 8 and 9. This can be attributed to the higher reinforcement ratio of the former slabs as well as the successful prevention of bond slip failure.

In terms of capacity, figures 8 and 9 show a significant load capacity increase for slabs reinforced with CFRP flexural bars (34.7 % load enhancement in slab SC1 over SG1 and 16.97 % and 33.76 % in slab SC2 over SG2 and SG3, respectively). This is due to the higher modulus of elasticity of the CFRP material, which leads to a larger area of concrete in compression. A slight increase in the capacity of the slabs reinforced with shear reinforcement is also seen. In fact, a 16.5 % and 13.92 % load enhancements are achieved in slabs SGS1 and SGS2 over SG1 and SG3, respectively. The higher capacity of slab SGS1 over slab SG1 can be attributed to the role of the shear reinforcement in delaying bond slip. However, in case of slab SGS2, the capacity enhancement is due to the role of the shear reinforcement in preventing punching shear failure at lower load levels.

The ineffectiveness of the shear reinforcement to prevent totally the punching shear failure of slab SGS2 may be attributed to the brittleness of the CFRP material of the “Shearband”. This brittleness is believed to result in problems not expected with a ductile material like steel. This is because when failure occurs in one of the vertical legs of the ‘Shearband’, no redistribution of

stress and load can occur and all the other vertical legs can fail successively. This implies that a higher partial safety factor or reduced material strength should be used when designing with brittle shear reinforcement.

PREDICTIVE APPROACHES FOR CONCRETE SHEAR RESISTANCE

For determining the concrete shear resistance of FRP RC flat slabs, the strain, stress and modified approaches are investigated. These three approaches mainly modify the actual area of the flexural tension FRP reinforcement 'A_{FRP}' into an equivalent steel area 'A_s', for use in code equations, in order to take into account the different material properties of FRP when compared to conventional steel. The differences between the three approaches lie in the method of calculation of A_s.

Table 1 shows the experimental, as well as, the predicted capacities of the tested slabs according to the three approaches investigated, based on BS 8110 code equations (1985). In this table, both maximum and average experimental stress values ($\sigma_{max.}$ and $\sigma_{avg.}$) in the flexural reinforcement at failure are shown together with the experimental failure loads. In addition, σ_{pFRP} in the stress approach, represents the predicted stress in the flexural reinforcement at which punching shear failure is predicted. This represents the point of intersection of the punching shear capacity curve, according to the stress approach, with the flexural capacity curve obtained from a simple section analysis program.

Strain approach

This approach represents the basis upon which most equations calculating the concrete shear resistance are currently modified to incorporate FRP reinforcement. The premise in this approach is that the concrete section does not actually recognize what it is reinforced with, but only experiences forces and strains. Hence, if the design using FRP reinforcement maintains the same strain when the design forces are developed, then that design will by definition lead to the same result, i.e. a safe design. For this reason, Clarke (1996) and the Institution of Structural Engineers in the UK (1999) recommended the use of an equivalent area of steel 'A_s' in table 3.9 of BS 8110 (1985), for determining the concrete shear resistance, by multiplying the actual area of FRP reinforcement 'A_{FRP}' by the modular ratio of FRP 'E_{FRP}' to that of steel 'E_s'.

The above implies that punching shear failure will occur when both the force and strain in the flexural FRP reinforcement are roughly the same as at yield for conventional reinforcement. The yield strain assumed for steel is 0.0025. The test results shown in table 1, for slabs SG2, SG3 and SC2, prove that this approach is conservative and hence, leads in a lower bound solution.

Stress approach

The equal stress approach assumes that the strain in the longitudinal reinforcement does not have an effect on the concrete shear resistance and, hence, considers just the design force (or stress) in the FRP reinforcement to be equivalent to that of steel reinforcement. This stress-based approach is proposed by the authors as an upper bound solution, since, when the same force is developed, the strain in the concrete and FRP flexural reinforcement is much higher than the corresponding

strain in steel. The modified value for the equivalent area of steel can only be obtained by finding the stress 'σ_{pFRP}' at the load where the punching shear capacity curve intersects the flexural capacity curve. Hence, the area of steel is modified by multiplying the actual area of FRP reinforcement 'A_{FRP}' by the stress ratio 'σ_{pFRP}' to that of steel yield stress 'σ_y' (taken as 460 MPa for BS 8110).

Results using the stress approach are shown in table 1 for the tested FRP RC flat slabs and confirm that this approach provides an upper limit of the punching shear capacity.

Modified approach

Having established upper and lower limits, the authors [El-Ghandour, Pilakoutas and Waldron (1999a, b and c)] have developed a new proposal based on the experimental work of flat slab testing carried out in this study. This approach takes partial advantage of the force that can be developed by FRP reinforcement beyond the lower bound strain limit to a new value of 0.0045. According to this approach, the equivalent area of steel is obtained as in the case of the strain approach, multiplied by a correction factor $\phi_\varepsilon = 1.8$. Hence, the area of steel is modified by:

$$A_s = A_{FRP} (E_{FRP} / E_s) (\phi_\varepsilon) \qquad (1)$$

where,

ϕ_ε is a correction factor equal to $\varepsilon_{FRP} / \varepsilon_y$

ε_{FRP} is the maximum strain allowed in the flexural reinforcement (proposed 0.0045),

ε_y is the yield strain of steel (taken as 0.0025 for BS 8110).

Results shown in table 1 prove that this modified approach gives accurate punching shear capacity predictions for both GFRP and CFRP RC flat slabs which failed in punching shear.

Figures 10 and 11 show the experimental punching shear capacities of slabs SG3 and SC2, respectively, when plotted against the experimental maximum and average stresses in the flexural bars in the critical region, as well as the stress in the critical section predicted by section analysis. The critical region of the tested slabs is defined as the central region around the column in which punching shear failure occurs. The figures also show the punching shear capacity predictions according to the three approaches, when applied to the BS 8110 code equation (1985). The strain and modified approaches are represented by horizontal lines, since they only predict the ultimate load. The value of stress, σ_{pFRP}, required by the stress approach is obtained by finding the point at which the punching shear capacity curve intersects the expected flexural capacity curve. From those figures, it is obvious that the modified approach is the most accurate one for punching shear capacity predictions.

Verification of the modified approach

The validity of the modified approach was checked by comparisons with test results of another study by Matthys and Taerwe (1997). Figure 12 shows comparisons of the test results with both the strain and modified approach predictions. The results were modified to account for the higher concrete strength expected at the time of testing. In this figure, series C, CS and H represent slabs

reinforced with CFRP NEFMAC grids, CFRP mesh with sanded surface bars and hybrid type of FRP NEFMAC grids comprising both glass and carbon fibres. From this figure, it can be seen that the strain approach is again conservative, while the modified approach is more accurate in punching shear capacity predictions.

DESIGN APPROACH FOR FRP SHEAR REINFORCEMENT

The provision of shear reinforcement in RC flat slabs is also subject to strain restrictions when using FRP reinforcement. The strain approach imposes the limit of 0.0025, which corresponds to the strain at which steel bars normally yield.

However, by studying slab SGS2 with CFRP shear reinforcement (table 1), it is seen that punching shear failure occurred at an average stress level of 446 MPa in the CFRP shear reinforcement. Hence, it is proposed that the strain limit is relaxed by using a multiplication factor of 1.8 [El-Ghandour, Pilakoutas and Waldron (1999a)]. It should be noted that the experimental strain levels obtained from the other two slabs with shear reinforcement (SGS1 and SCS1) cannot be used directly due to premature bond slip failure.

For slab SGS2 which failed in punching shear, table 1 shows that the strain approach capacity prediction is only slightly above the experimental one, despite the fact that both major assumptions of the strain approach were violated. Firstly, the experimental value of strain in the shear reinforcement of 0.0041 exceeded the design value of 0.0025, and secondly, the strain in the FRP flexural bars also exceeded the value of 0.0025, which means that the strain approach underestimates both the contribution of shear reinforcement and that of concrete. Since by adding

two conservative estimations for the concrete shear resistance and shear reinforcement contribution the result still overestimates the slab capacity, this implies that the assumption that concrete contributes fully to the punching shear resistance once a punching shear crack is formed (i.e. adding the full concrete shear resistance to the reinforcement contribution), is not valid.

In order to determine the actual amount of concrete contribution to the punching shear resistance, the experimental failure loads and average strains in the shear reinforcement for slabs SGS1, SCS1 and SGS2 are used, as shown in table 2. In this table, $\varepsilon_{avg,\ sh}$ and $\sigma_{avg,\ sh}$ represent the average experimental strains and stresses in the shear reinforcement at failure, respectively. P_{FRPs} represents the actual shear reinforcement contribution to the overall capacity of the slabs according to the average experimental stresses ($\sigma_{avg,\ sh}$). P_{FRP} represents the experimental failure loads of the slabs. P_c represents the actual concrete contribution to the overall capacity of the slabs and is calculated as the difference between P_{FRP} and P_{FRPs}. P_{cmod} represents the predicted concrete contribution to the overall capacity of the slabs according to the modified approach, which is capable of accurately predicting the concrete shear resistance as shown earlier. Consequently, the ratio P_c/P_{cmod} represents the actual fraction of the full concrete shear resistance that contributes to the overall slab capacity at failure.

From table 2, it can be seen that the actual fractions of the full concrete shear resistances that contributed to the overall capacities of the tested slabs were 0.8, 0.6 and 0.55 for slabs SGS1, SCS1 and SGS2, respectively. Hence, it is obvious that, even in slabs SGS1 and SCS1 which failed in bond slip at loads lower than their punching shear capacities, the full concrete contribution to shear resistance was not maintained due to the effect of severe cracking. The

lowest concrete contribution is experienced in slab SGS2, which failed in punching shear. This seems reasonable since, in SGS2, the initiation of the punching shear cracks reduces dramatically the concrete shear resistance. Accordingly, it is accepted that the concrete contribution to the punching shear resistance is substantially reduced after the initiation of the major shear crack and it is proposed that only 50 % of the concrete shear resistance can be relied upon at this stage [El-Ghandour, Pilakoutas and Waldron (1999a)]. This is in line with the ideas of the ACI 318 (1995) code.

By using all the above proposals, the predicted capacities of the slabs are found to be 243, 265 and 272 kN for slabs SGS1, SCS1 and SGS2, respectively, as shown in table 1. Although the first two values are still overestimating the capacities of slabs SGS1 and SCS1, due to their bond slip failure, the third prediction for slab SGS2, which failed in punching shear, is in perfect agreement with the experimental value. However, further research is recommended in this area.

COMPARISON BETWEEN MODIFIED APPROACH, ACI 318-95, ACI 440-98 AND MODIFIED ACI PREDICTIONS

According to the ACI 318-95 code (1995), the punching shear capacity of RC flat slabs without shear reinforcement in case of a square internal column is calculated by the following equation (minimum of ACI 318-95 code equations 11-35, 11-36 and 11-37):

$$P_{ACI} = 1.33 (f_c')^{0.5} (c + d) d \quad (2)$$

where,

f_c' is the concrete cylinder strength in MPa

c is the side length of the column in mm

d is the effective depth in mm

From equation 2, it is obvious that the above ACI 318-95 code equation totally ignores the influence of tension flexural reinforcement when calculating the concrete shear resistance and depends heavily on concrete strength. This is not too unreasonable in the case of steel reinforcement, since with its high modulus of elasticity, the dominant factor determining concrete shear resistance will be the area of concrete in compression, which remains constant as the neutral axis depth does not vary much with normal steel reinforcement ratios. Hence, in case of steel, the ACI 318-95 equation gives good predictions though conservative at low levels of reinforcement. However, when using FRP reinforcement with low modulus of elasticity, the concrete shear resistance becomes more sensitive to the reinforcement stiffness, as the neutral axis depth reduces significantly with low reinforcement ratios. In such cases, the ACI 318-95 prediction becomes too unconservative.

The ACI Committee 440 (1998) proposed a modification based on the strain approach to account for the axial rigidity of FRP flexural reinforcement, as shown in equation 3:

$$P_{ACI} = [1.33 (f_c')^{0.5} (c + d) d] (E_{FRP} / E_s) \quad (3)$$

where,

E_{FRP} is the modulus of elasticity of FRP reinforcement in MPa

E_s is the modulus of elasticity of conventional steel MPa

Figure 13 shows comparisons between the experimental capacities of the slabs which failed in punching shear in this study and the predictions of the modified approach, the ACI 318-95 and the ACI 440-98. This figure confirms that the ACI 318-95 code overestimates the slab capacities, since it totally ignores the effect of the low stiffness FRP reinforcement. The figure also shows the very conservative predictions of the ACI 440-98 equation.

It is therefore proposed to modify the ACI 440-98 equation (3) by raising the term refferring to the reinforcement stiffness to the power of 0.33, as in the case of the BS 8110 code. Hence, the proposed equation for use with FRP reinforcement (in case of a square internal column) is:

$$P_{ACI} = [1.33 (f_c')^{0.5} (c + d) d] (E_{FRP} / E_s)^{0.33} \quad (4)$$

The modified ACI equation (4) predictions are checked against the results from this study and are found to be in good agreement, as shown in Figure 13.

CONCLUSIONS

The main flexural cracks developed directly above the longitudinal reinforcement of all slabs and led to bond splitting in the slabs with low reinforcement ratios.

The smaller flexural bar spacing in the second phase of slabs (SG2 to SGS2) eliminated the problems of concrete splitting and prevented the bond slip failure in these slabs, which failed in punching shear.

Much higher average strains are developed in the flexural reinforcement of slabs SG2 to SGS2, as well as, in the shear reinforcement of slab SGS2, at punching shear failure, when compared to the yield strain of conventional steel (0.0025). Hence, the strain limitations currently adopted appear to be very conservative.

A modified strain approach for calculating the concrete shear resistance is proposed and was demonstrated to accurately predict the punching shear capacities of FRP RC flat slabs.

The punching shear capacity of FRP RC slabs with FRP shear reinforcement is most accurately predicted by halving the calculated concrete contribution of the modified approach. For the shear reinforcement, the strain limit of 0.0045 is proposed. The maximum spacing for shear reinforcement is also proposed to be 0.5d.

The ACI 318-95 code overestimates the concrete shear resistance of FRP RC flat slabs with low reinforcement ratios. On the other hand, the ACI 440-98 equation highly underestimates the concrete shear resistance of FRP RC flat slabs.

A modified ACI equation for calculating the concrete shear resistance is proposed based on a stiffness correction factor $(E_{FRP} / E_s)^{0.33}$ and is found to accurately predict the punching shear capacity of slabs tested in this study.

AKNOWLEDGEMENT

The authors wish to acknowledge the support of the Eurocrete project for technical and material support and the European Commission for funding the TMR Network 'Confibrecrete'.

REFERENCES

Achillides, Z., Pilakoutas, K. and Waldron, P., 'Bond Behaviour of FRP Bars to Concrete' Proceedings of the Third International Symposium on Non-Metallic (FRP) Reinforcement for Concrete Structures FRPRCS-3, Published by Japan Concrete Institute, Sapporo, October 1997, Volume 2, pp.341-348.

ACI, 'Building Code Requirements for Reinforced Concrete and Commentary (ACI 318-95/ACI 318R-95)' American Concrete Institute Committee 318, Detroit, 1995, 353 pp.

ACI, 'Provisional Design Recommendations for Concrete Reinforced with FRP Bars (ACI 440R-98)' American Concrete Institute Committee 440, Farmington Hills, Michigan, Draft 2, September, 1998, section 6.5.

BS 8110, 'Code of Practice for Design and Construction' British Standards Institution, Part 1, British Standards Institution, London, 1985, 124pp.

Clarke, J. L., 'Modification of Design Rules to Incorporate Non-ferrous Reinforcement' Report No. 1, Sir William Halcrow & Partners Ltd, January, 1996, 34 pp.

El-Ghandour, A. W., 'Behaviour and Design of FRP RC Slabs' PhD Thesis, Department of Civil and Structural Engineering, University of Sheffield, UK, October 1999, 285 pp.

El-Ghandour, A. W., Pilakoutas, K. and Waldron, P., 'Behaviour of FRP Reinforced Concrete Flat Slabs' Proceedings of the Third International Symposium on Non-Metallic (FRP) Reinforcement for Concrete Structures FRPRCS-3, Published by Japan Concrete Institute, Sapporo, October 1997, Volume 2, pp.567-574.

El-Ghandour, A. W., Pilakoutas, K. and Waldron, P., 'Behaviour of FRP Flat Slabs with CFRP Shear Reinforcement' Proceedings of the 8th European Conference on Composite Materials ECCM-8, Edited by Crivelli Visconti, I., Naples, Italy, June 1998, Volume 2, pp.399-406.

El-Ghandour, A. W., Pilakoutas, K. and Waldron, P., 'Punching Shear Design of FRP Reinforced Concrete Flat Slabs' TMR European Research Network 'ConFibreCrete' Seminar on Design Guidelines for FRP Reinforced Concrete Structures, Sintra, Portugal, January 18, 1999a.

El-Ghandour, A. W., Pilakoutas, K. and Waldron, P., 'Development of Design Guidelines for FRP Reinforced Concrete' Proceedings of the Second Middle East Symposium on Structural Composites for Infrastructure Applications, Edited by Hosny, A., Mahfouz, I. and Sarkani, S., Hurghada, Egypt, April 1999b, pp. 200 - 213.

El-Ghandour, A. W., Pilakoutas, K. and Waldron, P., 'New Approach for the Punching Shear Capacity Prediction of FRP RC Flat Slabs' Proceedings of the Fourth International Symposium

on Fibre Reinforced Polymer Reinforcement for Reinforced Concrete Structures, FRPRCS-4, Baltimore, Maryland, USA, 31 October to 5 November, 1999c, pp. 135 - 144.

Institution of Structural Engineers, 'Interim Guidance on the Design of Reinforced Concrete Structures Using Fibre Composite Reinforcement' The Institution of Structural Engineers, London, UK, August 1999.

Li, X., 'Punching Shear Resistance of RC Flat Slabs' PhD Thesis, Department of Civil and Structural Engineering, the University of Sheffield, UK, June 1997, 279 pp.

Li, X. and Pilakoutas, K., 'Alternative Shear Reinforcement in Flat Slabs' Report No. CCC/94/0030A, Centre for Cement and Concrete, Department of Civil and Structural Engineering, the University of Sheffield, March, 1995, 42 pp.

Matthys, S. and Taerwe, L., 'Punching Tests on Concrete Slabs Reinforced with FRP Grids' Proceedings of the 3rd International Symposium on Non-Metallic (FRP) Reinforcement for Concrete Structures (FRPRCS - 3), Published by Japan Concrete Institute, Sapporo, Japan, October 14 - 16, 1997, Volume 2, pp. 559 - 566.

Pilakoutas, K. and Li, X., 'Alternative Shear Reinforcement for Reinforced Concrete Flat Slabs' Journal of Structural Engineering, American Society of Civil Engineers, ASCE, December, 1999.

Sheard, P. A., Clarke, J. L., Dill, M. J., Hammersley, G. P. and Richardson, D. M., 'Eurocrete - Taking Account of Durability for Design of FRP Reinforced Concrete Structures' Proceedings of

the Third International Symposium on Non-Metallic (FRP) Reinforcement for Concrete Structures FRPRCS-3, Sapporo, October 1997, Volume 2, pp.75-82.

LIST OF TABLES

Table 1 Experimental and predicted punching shear capacities

Slab	f_{cu} avg MPa	ρ %	Experimental Results $\sigma_{max.}$ (MPa)	$\sigma_{avg.}$ (MPa)	Load (kN)	Type	Predictions based on BS 8110 Strain App. Load (kN)	Stress App. σ_{pFRP}	Stress App. Load(kN)	Mod. App. Load (kN)
SG1	40	0.18	405	373	170	Bond	151	-	-	184
SC1	41	0.15	698	526	229	Bond	205	-	-	249
SGS1	44	0.18	472 (209)*	339	198	Bond	238	-	-	243
SCS1	34	0.15	517 (346*)	440	200	Bond	274	-	-	265
SG2	58	0.38	418	318	271	P. Shear	224	650	415	273
SG3	38	0.38	360	332	237	P. Shear	194	533	340	237
SC2	37	0.35	627	508	317	P. Shear	260	616	355	316
SGS2	43	0.38	508 (649*)	384	270	P. Shear	286	-	-	272

* Values in brackets represent the stress in the shear reinforcement

Table 2 Concrete contribution to the slab capacity

Slab	Shear Reinforcement		P_{FRPs}	Slab Capacities		$P_c = P_{FRP} -$	$P_{cmod.}$	$P_c/P_{cmod.}$
	$\varepsilon_{avg.,\,sh}$	$\sigma_{avg.,\,sh}$ (MPa)	(kN)	P_{FRP} (kN)	Fail. Type	(kN)	(kN)	
SGS1	0.0014	154	46.2	198	Bond Slip	151.8	189	0.8
SCS1	0.002	222	66.6	200	Bond Slip	133.4	233	0.6
SGS2	0.0041	446	133.8	270	Punch. Shear	136.2	248	0.55

LIST OF FIGURES

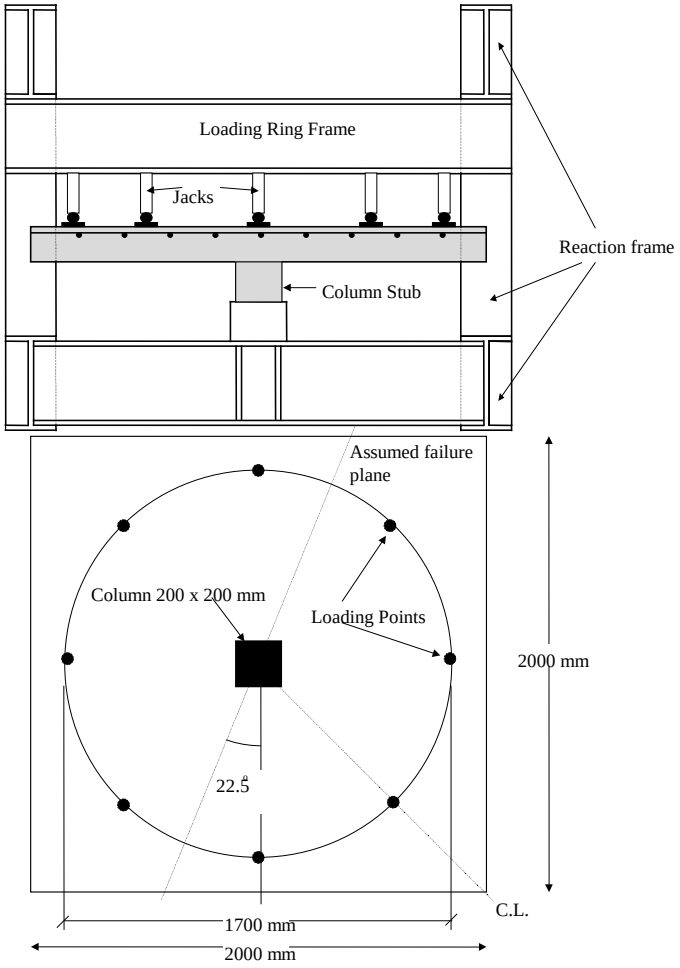

Figure 1 Slab geometry and schematic representation of test set-up

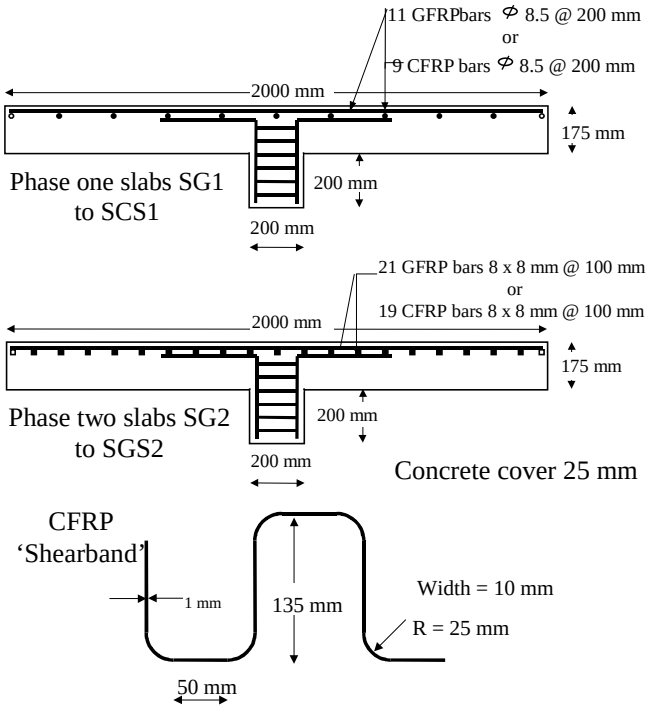

Figure 2 Slab layout and reinforcement details in the tested slabs

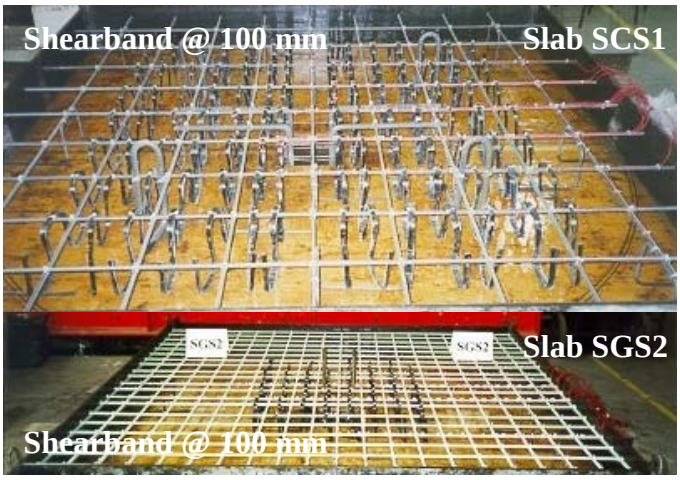

Figure 3 Distribution of shear reinforcement in SGS and SCS slabs

Figure 4 Crack localization in the slabs of the first phase

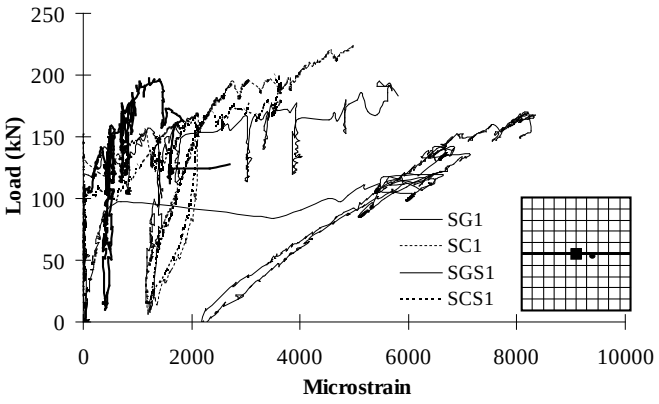

Figure 5 Load-reinforcement strain curves for phase one slabs

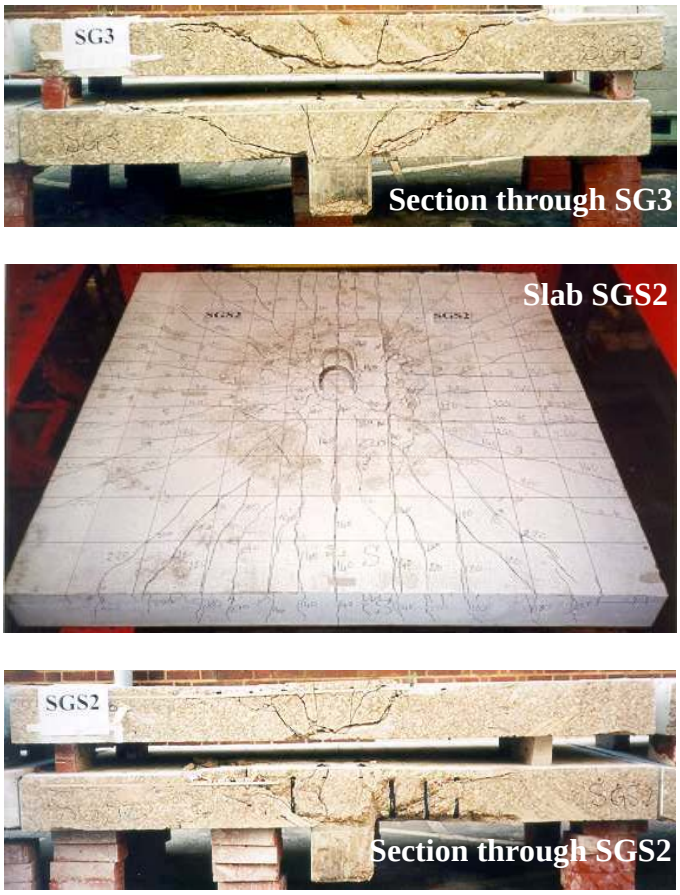

Figure 6 Punching shear failure of the slabs of the second phase

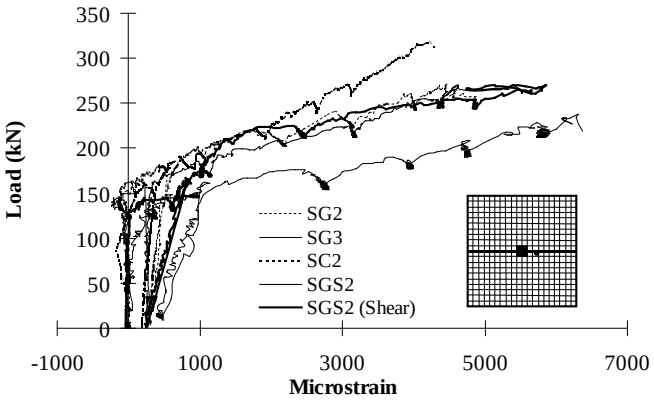

Figure 7 Load-reinforcement strain curves for phase two slabs

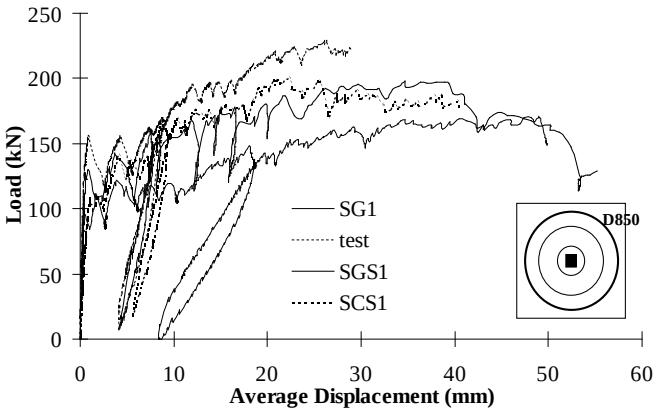

Figure 8 Average load-deflection curves at location D850 for phase one slabs

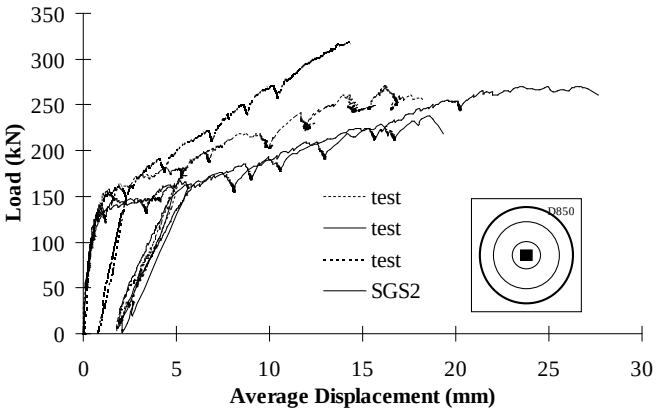

Figure 9 Average load-deflection curves at location D850 for phase two slabs

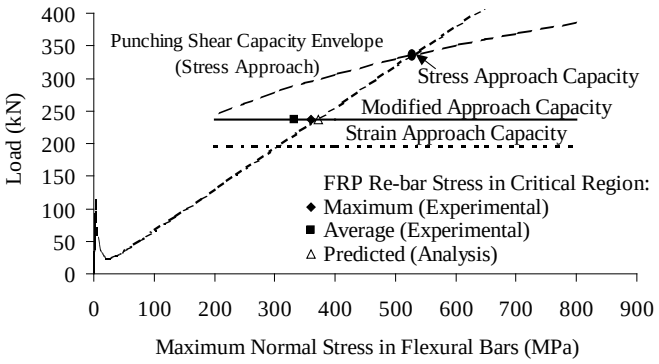

Figure 10 Experimental and predicted capacities of slab SG3

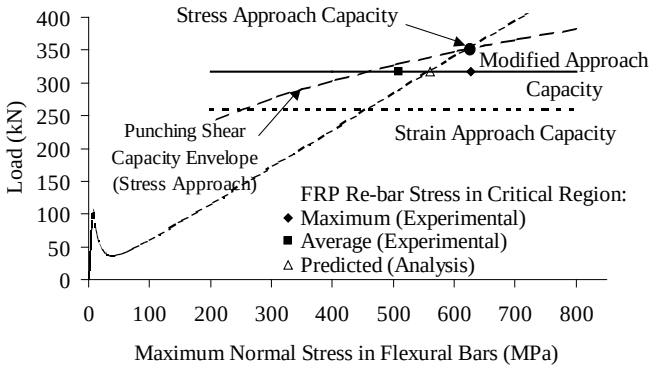

Figure 11 Experimental and predicted capacities of slab SC2

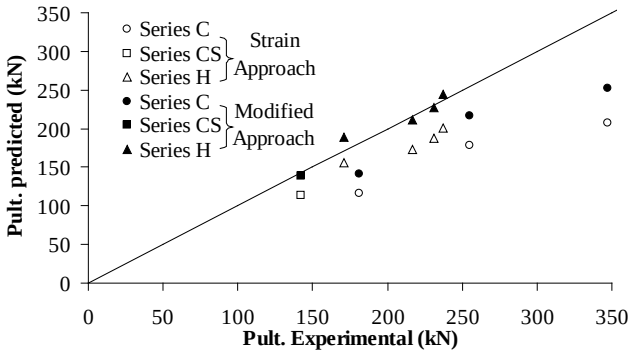

Figure 12 Strain and modified approaches predictions for slabs tested by Matthys et al. (1997)

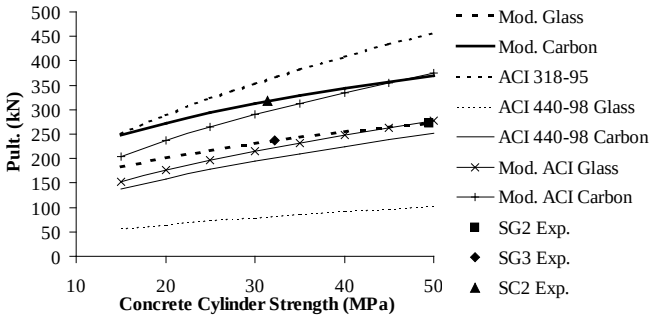

Figure 13 Normalised experimental and predicted capacities of slabs SG2, SG3 and SC2

LIST OF FIGURE LEGENDS